



Original Article

Knee meniscus regeneration using autogenous injection of uncultured adipose tissue-derived regenerative cells

Masakatsu Itose ^{a, b}, Tetsuo Suzawa ^{a, *}, Yo Shibata ^c, Shinsuke Ohba ^d, Koji Ishikawa ^e, Katsunori Inagaki ^e, Tatsuo Shirota ^b, Ryutaro Kamijo ^a^a Department of Biochemistry, School of Dentistry, Showa University, Tokyo, Japan^b Department of Oral and Maxillofacial Surgery, School of Dentistry, Showa University, Tokyo, Japan^c Department of Conservative Dentistry, Division of Biomaterials and Engineering, School of Dentistry, Showa University, Tokyo, Japan^d Department of Cell Biology, Institute of Biomedical Sciences, Nagasaki University, Nagasaki, Japan^e Department of Orthopaedic Surgery, School of Medicine, Showa University, Tokyo, Japan

ARTICLE INFO

Article history:

Received 11 March 2022

Received in revised form

18 August 2022

Accepted 12 September 2022

Keywords:

Adipose tissue-derived regenerative cells

Meniscus

Nanoindentation

Dynamic mechanical analysis

ABSTRACT

Introduction: The low healing potential of mature menisci necessitates traditional surgical removal (meniscectomy) to eliminate acute or chronic degenerative tears. However, removal of meniscal tissue is main factor causing osteoarthritis. Adipose tissue-derived regenerative cells (ADRCs), a heterogeneous cell population that includes multipotent adipose-derived stem cells and other progenitor cells, were easily isolated in large amounts from autologous adipose tissue, and same-day processing without culture or expansion was possible. This study investigated the regenerative potential of autologous ADRCs for use in meniscus defects.

Methods: In 10- to 12-week-old male SD rat partial meniscectomy model, an atelocollagen sponge scaffold without or with ADRCs (5.0×10^5 cells) was injected into each meniscus defect. Reconstructed menisci were subjected to histologic, and dynamic mechanical analyses.

Results: After 12 weeks, areas of regenerated meniscal tissue in the atelocollagen sponge scaffold in rats with ADRCs ($64.54 \pm 0.52\%$, $P < 0.05$, $n = 10$) were larger than in those without injection ($57.96 \pm 0.45\%$). ADRCs were shown capable of differentiating chondrocyte-like cells and meniscal tissue components such as type II collagen. Higher elastic moduli and lower fluid permeability of regenerated meniscal tissue demonstrated a favorable structure-function relationship required for native menisci, most likely in association with micron-scale porosity, with the lowest level for tissue integrity possibly reproducible.

Conclusions: This is the first report of meniscus regeneration induced by injection of ADRCs. The results indicate that ADRCs will be useful in future clinical cell-based therapy strategies, including as a cell source for reconstruction of damaged knee menisci.

© 2022, The Japanese Society for Regenerative Medicine. Production and hosting by Elsevier B.V. This is an open access article under the CC BY-NC-ND license (<http://creativecommons.org/licenses/by-nc-nd/4.0/>).

1. Introduction

Knee meniscus injuries are quite common in individuals affected by sports injury or aged knees, and known to cause knee

Abbreviations: ADRCs, adipose tissue-derived regenerative cells; ASCs, adipose-derived stem cells; MSCs, mesenchymal stem cells; SVFs, stromal vascular fractions; GFP, green fluorescent protein.

* Corresponding author. Department of Biochemistry, School of Dentistry, Showa University, 1-5-8 Hatanodai, Shinagawa, 142-8555 Tokyo, Japan. Tel: +81-3-3784-8163; Fax: +81-3-3784-5555

E-mail address: suzawa@dent.showa-u.ac.jp (T. Suzawa).

Peer review under responsibility of the Japanese Society for Regenerative Medicine.

<https://doi.org/10.1016/j.reth.2022.09.003>

2352-3204/© 2022, The Japanese Society for Regenerative Medicine. Production and hosting by Elsevier B.V. This is an open access article under the CC BY-NC-ND license (<http://creativecommons.org/licenses/by-nc-nd/4.0/>).

pain and swelling, as well as increased disability in relation to osteoarthritis development [1]. Meniscus blood supply and cellularity are age dependent, as the blood supply is fully vascularized in the infant stage, while in mature menisci it is nearly invisible, unless the outer portion is partly vascularized [2]. The low level of vascularization in mature menisci suggests a lower regeneration potential, hence partial removal of a meniscus tear is the most common arthroscopic procedure performed for a damaged knee joint. However, this traditional practice is far from ideal, as it has been shown to be correlated with degenerative changes in articular cartilage and progression of osteoarthritis [3,4]. A new regenerative strategy for defects in mature menisci would represent a significant clinical advance for treatment of meniscus injuries.

Tissue engineering using mesenchymal stem cells (MSCs) has been proposed as a strategy for meniscal reconstruction [5–7]. For example, a previous study that employed a rabbit model reported that implantation of bone-marrow derived MSCs resulted in marked regeneration of avascular meniscal tears with differentiated stable meniscus-like tissue [8]. Alternatively, adipose tissue is considered to be an abundant and accessible source of adult stem cells, which have an ability to differentiate along multiple lineage pathways [9]. Such adipose tissue is obtainable under local anesthesia with a minimum of patient discomfort [10,11]. Clinical-grade stromal vascular fractions (SVFs) of adipose tissue have been referred to as adipose-derived regenerative cells (ADRCs) [12], a heterogeneous cell population consisting of endothelial cells, fibroblasts, smooth muscle cells, macrophages, and adipose-derived stem cells (ASCs) [13,14]. On the other hand, ASCs increased IL-10 secretion by macrophages, suppressing inflammatory cytokine secretion, such as IL-1 α , TNF- α , and IFN- γ by M1 macrophages, and stimulated M2 macrophage phenotype activation [15]. ADRCs are reported to be multipotent progenitor cells that differentiate into

specific mesenchymal cell lineages, including bone, cartilage, tendon, fat, muscle, and early progenitors of neural cells, under certain conditions [16,17], while they also possess an ability to modulate immune responses. Unlike ASCs, which are expanded from SVFs by culturing, ADRCs can be used immediately in a single treatment session. Furthermore, the risks of infection and degeneration have been shown to be very low, because no culturing is necessary and establishment of a new cell processing center is also not needed. A number of reports regarding clinical applications of ADRCs have been published [18–21], with local injection thought to be a potential novel tissue engineering protocol for meniscus reconstruction.

In the present study, following a partial meniscectomy in rats, injection of an ADRC-embedded atelocollagen scaffold was performed. Atelocollagen is produced by telopeptides removal from natural collagen molecules [22], resulting in low antigenicity, and can be safely applied clinically for inducing chondrogenesis [23]. The mean pore size of atelocollagen scaffold was approximately 200 μ m, thus allowing for maximum reconstitution of meniscal

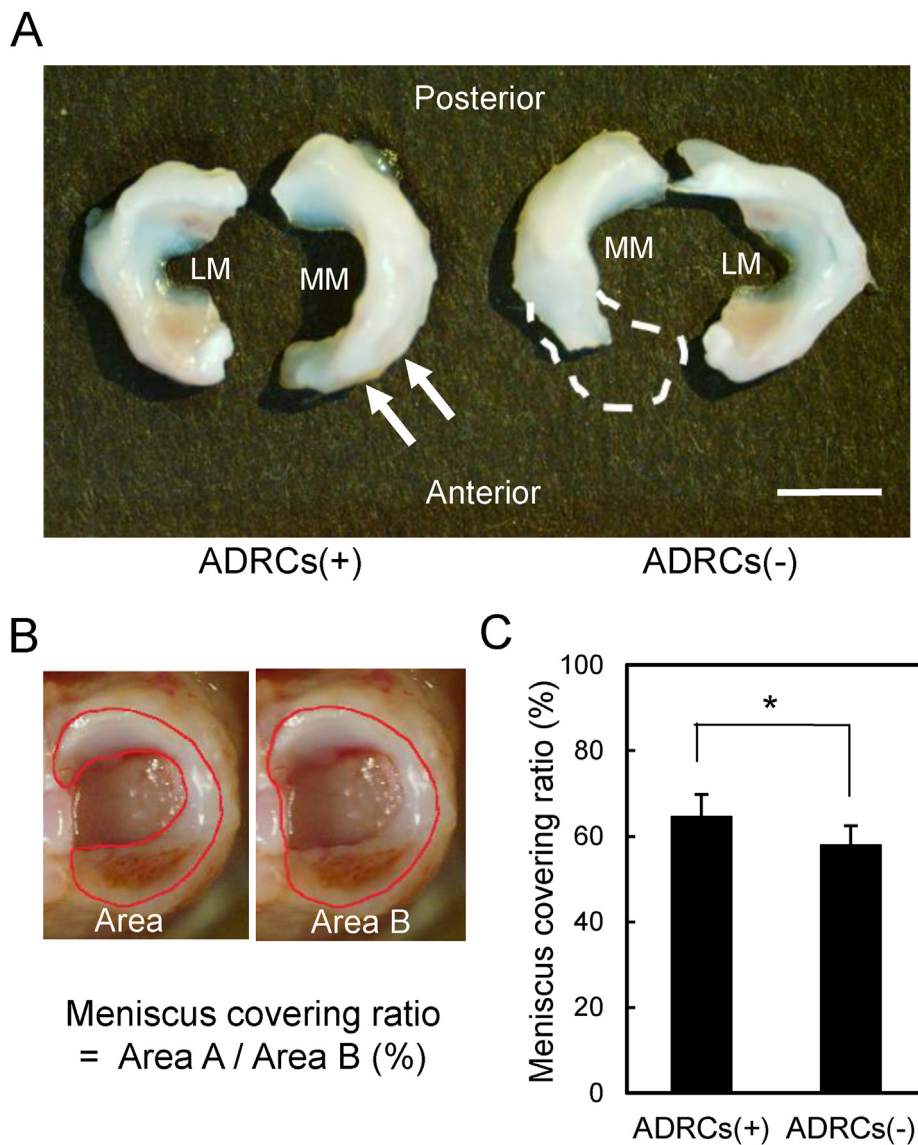


Fig. 1. Macroscopic observations of meniscal regeneration following intra-articular injection of ADRCs. (A) Microscopic findings of regenerated menisci at 12 weeks. White arrows indicate regenerated tissue. Scale bar = 3 mm. (B) The meniscus covering ratio, defined as ratio of the medial meniscus area (Area A: red line) to medial plateau area (Area B: red line), was calculated as follows: Area A/Area B. (C) The meniscus covering ratio was compared between the presence [ADRCs(+)] and absence of [ADRCs(-)] ADRCs. Bar shows mean \pm SD (n = 10). Data were analyzed using a Mann-Whitney U test (*p < 0.01). Abbreviations: MM, medial meniscus; LM, lateral meniscus.

tissues [24]. *In vivo* analysis of fibrocartilaginous tissue formation in meniscal tissue defects in the presence or absence of ADRCs was performed. In addition, the dynamic mechanical properties of regenerated and native meniscal tissues are examined.

2. Methods

2.1. Animals

Wild-type male Sprague Dawley (SD) (SLC Inc., Hamamatsu, Japan), green fluorescent protein (GFP)-transgenic [SD-Tg(CAG-EGFP)] (SLC Inc., Shizuoka, Japan), and F344/NJcl-*rnu/rnu* (CLEA Japan, Inc., Tokyo, Japan) male rats were used in the experiments. All procedures were approved by the Ethical Board for Animal Experiments of Showa University (approval no. 15062).

2.2. Preparation of rat adipose tissue derived from stem cell suspensions

Inguinal adipose tissues were obtained from 8- to 10-week-old male rats and digested with Celase® enzyme (Cytosol Therapeutics Inc. San Diego, CA, USA) for 40 min at 37 °C. The ADRC fraction was separated by centrifugation at 600×g for 5 min, then sequentially passed through Falcon® cell strainers (BD Bioscience, San Diego, CA, USA) with 100- and 40-μm sized pores.

2.3. Surgical procedures

Type I atelocollagen sponges (MIGHTY, size: ϕ 5 × 3 mm, mean pore size: 200 μm; KOKEN CO., LTD., Tsuruoka, Japan) were split

aseptically into small quarter-sized pieces with one-half thickness for use as a scaffold and sterilized by ultraviolet irradiation overnight before use. Harvested ADRCs were resuspended in type I atelocollagen gel (I-AC; KOKEN CO., LTD.) at a concentration of 5×10^7 cells/ml, then 10 μl of the cell suspension (5×10^5 cells) was impregnated into each atelocollagen scaffold by centrifugation (500×g, 1 min). The mean pore size of the atelocollagen scaffold was approximately 200 μm, which was considered necessary for maximizing embedded cell proliferation and extra-cellular matrix production, as recommended in a recent study [24].

Under isoflurane (1–1.5%) anesthesia, the bilateral hind limbs were shaved and an incision was made on the anterior side of the bilateral knees. The knee joint was exposed and the medial collateral ligaments were transected, then the anterior half of the medial meniscus was resected and removed at the level of the medial collateral ligament. It is known that resected menisci do not spontaneously heal. An atelocollagen sponge scaffold without or with ADRCs (5.0×10^5 cells) was placed on each meniscus defect. To clarify substantial reconstruction of meniscal tissue *in vivo*, we performed a partial meniscectomy on both sides of the SD rat knees (n = 10), then injected an autologous ADRC suspension (5.0×10^5 cells in 10 μl type I atelocollagen gel) into the intraarticular region of the right knee immediately before closing the incision. In the control group, the same volume of type I atelocollagen gel was injected into the left knee. To trace injected cells, ADRCs were harvested from male GFP-transgenic rats and injected into the knee of the male F344/NJcl-*rnu/rnu* rats.

The hind limbs of the rats were suspended for 1 week to mimic a non-weight bearing condition, then the proximal two-thirds of the

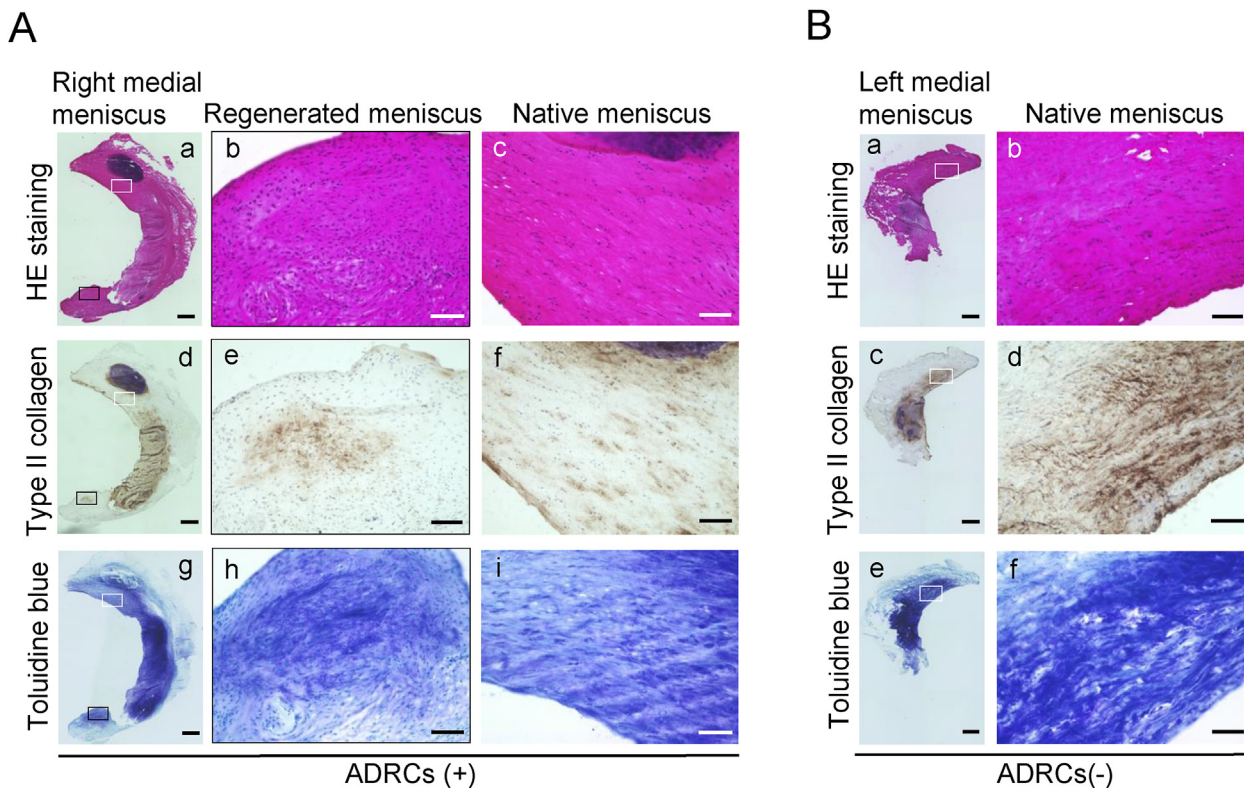


Fig. 2. Histological analysis of meniscal regeneration following intra-articular injection of ADRCs. (A) Representative tissue sections regenerated in presence of ADRCs [ADRCs(+) group] after staining with hematoxylin-eosin (top panel), immunostaining with type II collagen (middle panel), and staining with toluidine blue (bottom panel). Black square shows representative area during regeneration process. White square shows native meniscus. Scale bar = 500 μm (left panel). Scale bar = 100 μm (middle and right panel). (B) Representative sections in absence of ADRCs [ADRCs(-) group] after staining with hematoxylin-eosin (top panel), immunostaining with type II collagen (middle panel), and staining with toluidine blue (bottom panel). White square shows native meniscus. Scale bar = 500 μm (left panel). Scale bar = 100 μm (right panel).

tail was taped, with a swivel hook attached to the tape. Next, a string was passed through the hook and attached to the top of the animal cage. Due to the nature of the swivel hook, the rats had full access to food and water. After 1 week of hindlimb unloading, rats in all groups were allowed to walk freely, then euthanized at 4 or 12 weeks after the procedure.

2.4. Macroscopic observation

The tibial plateau with menisci was carefully separated from the femoral condyle and macroscopic images were obtained using fluorescence stereomicroscopy (MVX110; OLYMPUS, Tokyo, Japan), then the meniscus coverage ratio was calculated as described by Ozeki and colleagues [25].

2.5. Tissue preparation and histomorphometry analysis

For histology examinations, meniscus were harvested after 12 weeks, fixed in 4% paraformaldehyde for 3 days at 4 °C, and embedded in an optimal cutting temperature (OCT) compound (Sakura Finetek Japan, Tokyo, Japan). Meniscus were cut into 5- μ m thick horizontal sections, and stained with hematoxylin/eosin (HE) or Toluidine Blue staining.

2.6. Immunostaining

Following fixation, sections were blocked for 1 h at RT with 3% BSA/1% heat inactivated sheep serum/PBS with 0.1% TritonX-100 (PBST). Subsequently, they were incubated with the indicated primary antibody overnight at 4 °C, then washed 3 times with PBST and incubated for 1 h at RT with the secondary antibodies, and washed again 3 times with PBST. DAPI (0.5 μ g/ml in PBS) was used to visualize the nuclei. An anti-type II collagen antibody (mouse monoclonal antibody, Daiichi Fine Chemical CO. LTD, Toyama, Japan) and anti-GFP antibody (rabbit polyclonal antibody, Thermo Fisher Scientific, Rockford, IL, USA) were used as primary antibodies. The secondary antibodies were Alexa Fluor 488 and 546 (Thermo Fisher Scientific). For immunoenzyme staining, slides were first incubated with an anti-type II collagen antibody (Daiichi Fine Chemical CO. LTD) for 1 h at RT, followed by binding with secondary antibodies (goat anti-mouse IgG, Simple Stain MAX PO; Nichirei Biosciences, Tokyo, Japan), then 3,3'-diaminobenzidine (DAB) color development as well as hematoxylin counterstaining. Images were obtained with either a BIOREVO BZ-900 (KEYENCE, Osaka, Japan) or FV1200 BX61W1 (OLYMPUS, Tokyo, Japan) confocal laser scanning microscope.

2.7. Dynamic mechanical analysis

At 12 weeks after injection, the medial menisci ($n = 5$) were harvested and frozen in *n*-hexane and isopentane cooled with liquid nitrogen, and embedded in embedding medium (SCEM, Leica Microsystems GmbH, Wetzlar, Germany). The tissues were not subjected to any chemical fixation, as that would increase their elastic properties via conformational change of collagen molecules [26]. Frozen specimen blocks were affixed in the cryomicrotome stage and trimmed with a sharp tungsten carbide disposable blade (TC-65, Leica), then cross-sectioned in a longitudinal direction using a cryostat so that a fine surface was obtainable without the need for manual polishing. Each block surface was cut into 2-mm thick sections with a cryomicrotome (CM3050S, Leica). The remaining trimmed sample blocks were subjected to nanoindentation tests [27].

The samples were submerged in Hanks' balanced salt solution (Sigma-Aldrich) throughout the duration of nanoindentation testing. The nanoindentation experiments were performed using the central regions from both native and reconstructed meniscal tissues with a flat-end cylindrical tip (ϕ 50 μ m; Fig. 4A), utilizing a quantitative nanomechanical test instrument (TI 950 TriboIndenter, Hysitron, Inc., Eden Prairie, MN, USA). The distance between indents was always greater than 100 μ m. Force-displacement curves were recorded at a loading rate of 50 μ N/s to a maximum load of 500 μ N. The loading portion was followed by constant load holding at maximum load, to which sinusoidal dynamic indentations were superimposed. The applied amplitudes of the sinusoidal oscillations were 5 μ N at frequencies of 0.5–50 Hz within a single indentation (nanoDMAIII, Hysitron, Inc.). The 5- μ N force created an approximately 2-nm strain amplitude, which allowed for precise measurement of the stiffness of the material using dynamic indentation testing. During this period, the indenter tip simultaneously captured the frequency (strain-rate)-dependent tangent of phase lag ($\tan \delta$) and effective elastic modulus (storage modulus) values [28,29].

2.8. Statistical analysis

Meniscus coverage ratio was analyzed using a Mann-Whitney *U* test, with $p < 0.01$ considered to indicate significance. At least 5 indentations were evaluated using nanoindentation testing. Data were analyzed by ANOVA with a post-hoc Tukey's test ($p < 0.05$) and are expressed as the mean \pm SD.

3. Results

3.1. Meniscal regeneration after intra-articular injection of ADRCs

We performed a partial meniscectomy on SD rat knees, then injected an autologous ADRC suspension into the intraarticular region of knee immediately. After 12 weeks, areas of regenerated meniscal tissue in the atelocollagen sponge scaffold in rats with ADRCs [ADRCs(+)] group were larger as compared to those without injected ADRCs [ADRCs(-)] group (Fig. 1A). Quantification analysis demonstrated that the meniscus coverage ratio (Fig. 1B) was lower in the absence of ADRCs ($57.96 \pm 0.45\%$) as compared to that in their presence ($64.54 \pm 0.52\%$, $P < 0.05$, $n = 10$) (Fig. 1C).

3.2. Histological observation of meniscal regeneration after intra-articular injection of ADRCs

Following HE staining (Fig. 2A and B), observations of the restored portion showed it to have a fibrous cartilage-like organization. A small amount of atelocollagen sponge residue was observed as a red dye. The two-dimensional configuration of the cells in the regenerated menisci was similar to that of meniscal cells in native tissues (Fig. 2A, top panel). After 12 weeks in rats that received injection of ADRCs, the matrix in the inner portion of regenerated menisci was found to be stained with Toluidine blue and immunostained with type II collagen (Fig. 2A, middle and bottom panels). In contrast, no promotion of tissue repair was observed in the group without ADRC injection (Fig. 2B, top panel), including no Toluidine blue staining or immunostaining with type II collagen observed in those rats (Fig. 2B, middle and bottom panel). Type I collagen as a major component of fibrocartilage, was found throughout the matrix of meniscus. The distribution of type I collagen was nearly identical between native and regenerated menisci (data not shown).

3.3. Distribution of ADRCs in regenerated meniscal tissues

To trace injected cells, ADRCs from GFP transgenic rats were injected into nude rats that underwent a partial meniscectomy. GFP-positive (green) areas were detected in the ADRC group at 12 weeks after injection (Fig. 3Ac, Bb). GFP-positive cells were not observed in the absence of ADRCs (Fig. 3Ad, Bb), whereas they were observed at 4 (Fig. 3Ca-d) and 12 (Fig. 3Ce-h) weeks after transplantation in cross-sectioned samples that contained ADRCs. In addition, a number of GFP-positive cells remained visible on the surface of regenerated meniscal tissue after 12 weeks with concomitant growth of type II collagen. However, the presence of GFP-positive ADRCs was not always seen in concurrence with type II collagen expression.

3.4. Dynamic mechanical properties of regenerated tissues as compared to those of native meniscus tissues

The viscoelastic $\tan \delta$ value at the lowest frequency of the native meniscal tissues was significantly higher ($p < 0.05$) as compared to the regenerated tissues (Fig. 4B). Both types of surfaces generated non-linear viscoelasticity during dynamic indentation testing with a flat-end cylindrical tip (Fig. 4A). Furthermore, storage moduli observed on the meniscal tissues were significantly increased ($p < 0.05$) with the dynamic amplitudes (strain-rate stiffening). Although the corrected elastic moduli (storage moduli) value for each sample surface showed strain-rate stiffening against dynamic frequencies, storage moduli, which ranged from 0.5 to 50 Hz on the regenerated tissues, were nearly 10-fold greater as compared to those on native tissues ($p < 0.05$) (Fig. 4C). Despite the large

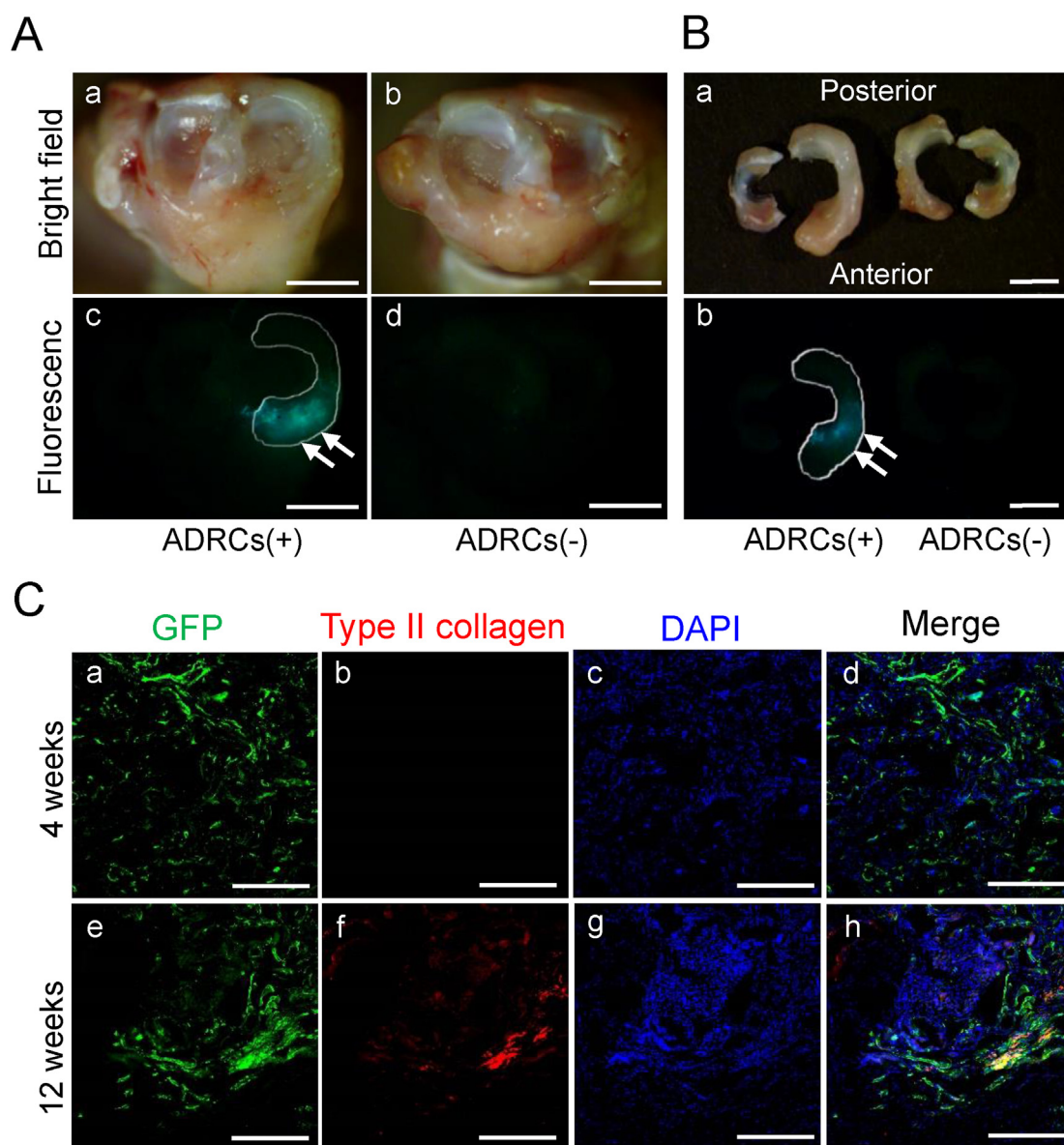


Fig. 3. Macroscopic observations of meniscal regeneration following intra-articular injection of ADRCs derived from GFP transgenic rats. (A, B) Obtained menisci were examined using fluorescence stereomicroscopy. Top panel shows bright-field image and bottom panel a corresponding fluorescence image. White dotted line indicates native medial meniscus areas. White arrows indicate regenerated tissue (green). (A) Representative macroscopic findings of tibial joint obtained after 12 weeks in presence [ADRCs(+)] (right foot) or absence [ADRCs(-)] groups of ADRCs (left foot). (B) Meniscus after separation from tibial joint [ADRCs(+): left side, ADRCs(-): right side]. (C) Representative double-immunohistochemical findings for GFP (green) and type II collagen (red) at 4 and 12 weeks after injection of ADRCs. Nuclei were stained with DAPI. Scale bar = 3 mm (A, B), Scale bar = 100 μm (C).

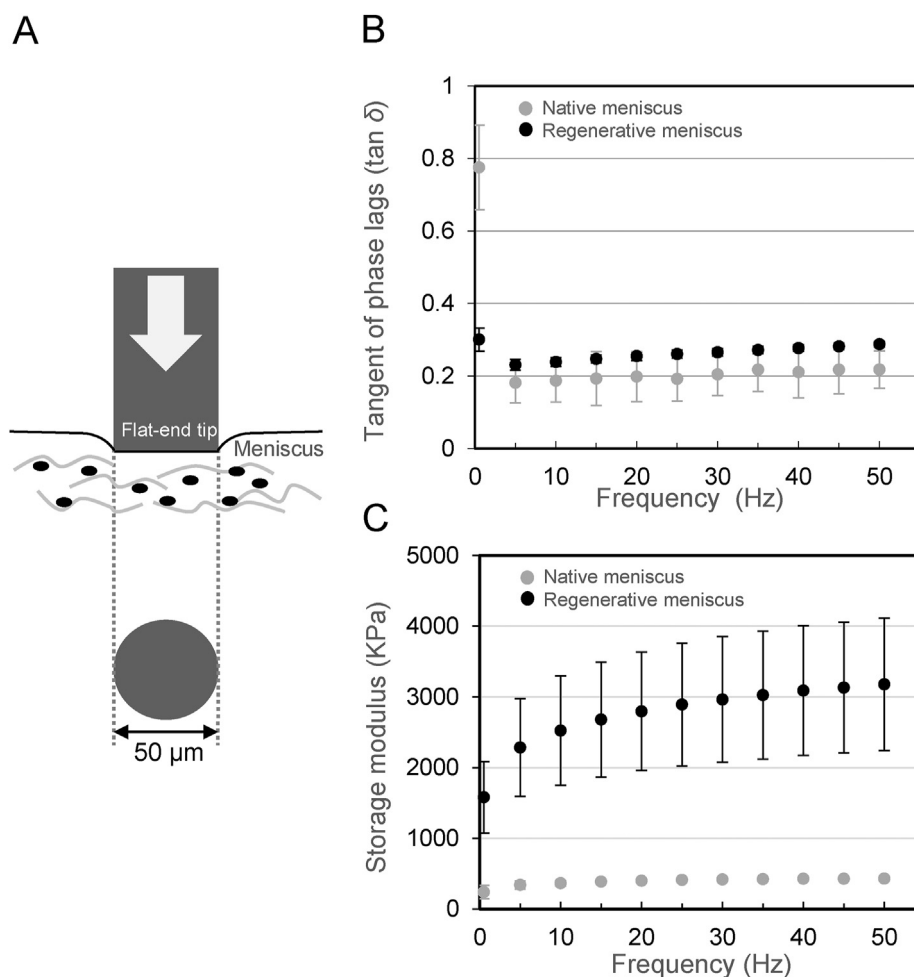


Fig. 4. Dynamic mechanical properties of regenerated tissues. (A) Schematic representation of findings obtained with nanoindentation testing of meniscus tissues using a flat-end tip. Values for (B) viscoelastic $\tan \delta$ and (C) storage moduli of regenerated meniscal tissues as compared to native tissues at each dynamic frequency (ranging from 0.5 to 50 Hz). Error bars show mean \pm SD (n = 5). Data were analyzed by ANOVA with a post-hoc Tukey's-test ($p < 0.05$).

reduction in $\tan \delta$ at 5 Hz on the regenerated tissues, the value bottomed out and then increased steadily ($p < 0.05$) up to the highest frequency of 50 Hz.

4. Discussion

The present study was conducted to investigate a novel tissue engineering protocol for treatment of meniscus defects by use of local injection of ADRCs embedded in an atelocollagen scaffold. Although several studies have reported that ASCs can be used as a cell source for tissue engineering, those require culturing for expansion to obtain an adequate number. In contrast, ADRCs are freshly isolated stem cells obtained from fat tissue by enzymatic digestion and can be used immediately after isolation in clinical situations without the need for culturing in a cell processing center. Katagiri et al. recently reported histological findings indicating that the distribution of matrix positive for type II collagen was different between native and regenerated menisci after 12 weeks [30]. They found that the peripheral area of native meniscus tissues was positive for type II collagen, while that area in the regenerated tissues was mostly negative for that, and suggested that regenerated meniscus tissues were not yet fully mature at 12 weeks after transplantation. Our findings are in agreement with those, as we observed that the peripheral areas of regenerated menisci were negative for type II collagen, whereas the inner portions were positive (Fig. 2A).

Although regenerated meniscal tissues were found to be highly saturated with GFP-positive cells, our microscopic observations showed that existing GFP-positive ADRCs did not always co-exist in regenerated meniscal tissues with expression of type II collagen. Several types of cells secrete factors such as BMP2, insulin-like growth factor-1, transforming growth factor- β 1, and basic fibroblastic growth factor, which have been shown to contribute to chondrocyte proliferation and meniscus development [31,32], thus autocrine and/or paracrine effects of ADRCs plus native cells via ASC secretion may be the principal causes of meniscal tissue regeneration at the surgical site. It is therefore considered that regeneration of menisci may be induced by not only the direct effect of ADRCs on surrounding cells, but also indirectly by the effects of growth factors. In future studies it will be important to analyze the meniscus forming capacity of ADRCs in a medial knee meniscus defect model, as that may provide a more beneficial environment for stable chondrogenic differentiation of ADRCs over a longer time period.

As for the dynamic mechanical properties of regenerated meniscal tissues as compared to native tissues, both types showed strain-rate stiffening and large viscoelasticity that occurred in parallel. Biological tissues often have effects on size-dependent mechanical properties [29]. Use of a greater than micron-scale contact area between the sample surface and flat-end cylindrical tip (ϕ 50 μ m) allowed for the present nanoindentation tests to

simultaneously capture dynamic mechanical responses of the tissues partly associated with micron-scale structures, indicating porosity. According to poroelastic theory, strain-rate stiffening of soft biological tissues can be interpreted as a dilatant response to an instantaneous increase in pore pressure [28]. With shear displacement, most materials have a tendency to expand in a direction perpendicular to the surface. In the present study, substantial shear strain was generated in meniscal tissues in response to penetration by the indenter tip, especially during cyclic oscillations, indicating a dynamic frequency.

Although regenerated meniscal tissues showed strain-rate stiffening, the values for the storage moduli on regenerated tissues were much higher as compared to the native meniscal tissues throughout the period of dynamic indentation testing. Assuming that the lowest level of tissue integrity in both native and regenerated tissues was nearly equivalent, such excessive storage moduli shown by the regenerated tissues were likely related to impaired micron-structural integrity. More specifically, lower porosity in regenerated tissue might enhance inelasticity, based on the theoretical prediction that an elastic modulus is predominantly determined by volume fraction and porosity [28].

Aside from their foundational inelastic stiffness, soft biological tissues, such as articular cartilage and knee meniscus, accommodate large amounts of joint load. To accomplish this, these tissues have a complex multi-phase structure composed of water and macromolecules [33]. Based on wet weight, the meniscus is highly hydrated (72% water), with the remaining 28% comprised of organic matter, primarily type II collagen and proteoglycan [34]. The large amount of water absorption by meniscus tissues is of particular importance with respect to the large amount of strain released via viscus damping loss, allowing for adaptation to changes in joint motion and pressure. Viscoelastic materials have often been represented as a viscous dashpot and elastic spring in previously reported studies [35]. When strain is applied to a viscoelastic material, a delayed viscus motion by the dashpot (fluid motion) dissipates the strain energy. Unlike calcified tissues, meniscal tissues are not able to bear a large amount of strain energy by pure elastic (time-independent) damping alone because of the extremely lower level of storage moduli, thus time-dependent viscoelasticity is an important determinant for their mechanical integrity. The higher level of viscoelasticity ($\tan \delta$) seen at the lowest dynamic frequency also represents the estimated higher porosity of native meniscus tissues, implying the inverse, namely, lower viscus motion in relation to lower porosity expected in regenerated meniscal tissues. Moreover, it is likely that the lower level of permeability of the structure inhibits the flow of fluid back to the deformed area, thus the viscoelastic $\tan \delta$ value for regenerated meniscal tissues steadily increases with cyclic loading, as strain diffusion is an alternative result of local structural changes. This suggests that any impaired mechanical property in regenerated tissue cannot be simply observed, but rather appropriate three-dimensional reconstruction at the micron level is needed so as to reproduce the mechanical integrity of the native meniscus. The micro-environment of the extracellular matrix plays an important role in regulating cell behavior, which may provide a proper micron-sized structure in regenerated tissues [36]. In this respect, further modifications of the engineered scaffold used in the present study should be considered along with caution regarding the micromechanical integrity of regenerated meniscal tissues.

5. Conclusion

In the present study, a novel procedure for meniscus regeneration was successfully established by combining ADRCs with an

atelocollagen scaffold. ADRC injection is a promising technique for meniscus tissue engineering, though it does not completely reproduce a proper structure–function relationship, as observed in native menisci at the micron level. The present findings also demonstrate a precise protocol for measurements of dynamic mechanical properties, such as viscoelastic and/or poroelastic properties of regenerated meniscal tissues.

Authors' contributions

All authors were involved in drafting the article or revising it critically for important intellectual content, and each approved the final version submitted for publication.

MI: Study concept and design, acquisition of data, data analysis, and manuscript writing. TSu: Study concept and design, data analysis, manuscript writing, and final approval of manuscript. YS: Acquisition of data, data analysis, and manuscript writing. SO: Analysis and interpretation of data. KIs and KIn: Study concept and design, and data analysis. TSh: Data analysis and manuscript revising. RK: Study concept and design, financial support, and manuscript revising.

Funding

This study was supported in part by The Project to Establish Strategic Research Center for Innovative Dentistry by the Ministry of Education, Culture, Sports, Science and Technology of Japan, 2011–2016, and by JSPS KAKENHI-Grant Number 19K19244.

Declaration of competing interest

None of the authors have conflicts of interest related to this work to declare.

Acknowledgments

We thank all members of the Department of Biochemistry, School of Dentistry, Showa University, for their valuable discussion.

References

- [1] Rongen JJ, van Tienen TG, van Bochove B, Grijpma DW, Buma P. Biomaterials in search of a meniscus substitute. *Biomaterials* 2014;35:3527–40.
- [2] Lotz MK, Otsuki S, Grogan SP, Sah R, Terkeltaub R, D'Lima D. Cartilage cell clusters. *Arthritis Rheum* 2010;62:2206–18.
- [3] Seedhom B, Hargreaves D. Transmission of the load in the knee joint with special reference to the role of the meniscus. Part I-II. *Eng Med* 1979;4:207–28.
- [4] Englund M, Lohmander LS. Risk factors for symptomatic knee osteoarthritis fifteen to twenty-two years after meniscectomy. *Arthritis Rheum* 2004;50:2811–9.
- [5] Caplan AL. Adult mesenchymal stem cells for tissue engineering versus regenerative medicine. *J Cell Physiol* 2007;213:341–7.
- [6] Caplan AL, Dennis JE. Mesenchymal stem cells as trophic mediators. *J Cell Biochem* 2006;98:1076–84.
- [7] Murphy JM, Fink DJ, Hunziker EB, Barry FP. Stem cell therapy in a Caprine model of osteoarthritis. *Arthritis Rheum* 2003;48:3464–74.
- [8] Zellner J, Hierl K, Mueller M, Pfeifer C, Berner A, Dienstknacht T, et al. Stem cell-based tissue-engineering for treatment of meniscal tears in the avascular zone. *J Biomed Mater Res B* 2013;101:1133–42.
- [9] Gimble JM, Katz AJ, Bunnell BA. Adipose-derived stem cells for regenerative medicine. *Circ Res* 2007;100:1249–60.
- [10] Lee RH, Kim B, Choi I, Kim H, Choi HS, Suh K, et al. Characterization and expression analysis of mesenchymal stem cells from human bone marrow and adipose tissue. *Cell Physiol Biochem* 2004;14:311–24.
- [11] Dicker A, Le Blanc K, Aström G, van Harmelen V, Götherström C, Blomqvist L, et al. Functional studies of mesenchymal stem cells derived from adult human adipose tissue. *Exp Cell Res* 2005;308:283–90.
- [12] Fraser JK, Hicok KC, Shanahan R, Zhu M, Miller S, Arm DM. The celution® system: automated processing of adiposederived regenerative cells in a functionally closed system. *Adv Wound Care* 2014;3:38–45.

- [13] Zuk PA, Zhu M, Ashjian P, De Ugarte DA, Huang JJ, Mizuno H, et al. Human adipose tissue is a source of multipotent stem cells. *Mol Biol Cell* 2002;13:4279–95.
- [14] Kokai LE, Marra K, Rubin JP. Adipose stem cells: biology and clinical applications for tissue repair and regeneration. *Transl Res* 2014;163:399–408.
- [15] Adutler-Lieber S, Ben-Mordechai T, Naftali-Shani N, Loberman D, Leor J, Asher E, et al. Human macrophage regulation via interaction with cardiac adipose tissue-derived mesenchymal stromal cells. *J Cardiovasc Pharmacol* 2012;18:78–86.
- [16] Minguell JJ, Erices A, Conget P. Mesenchymal stem cells. *Exp Biol Med* (Maywood). 2001;226:507–20.
- [17] Izadpanah R, Trygg C, Patel B, Kriedt C, Dufour J, Gimble JM, et al. Biologic properties of mesenchymal stem cells derived from bone marrow and adipose tissue. *J Cell Physiol* 2006;207:331–9.
- [18] Yoshimura K, Asano Y, Aoi N, Kurita M, Oshima Y, Sato K, et al. Progenitor-enriched adipose tissue transplantation as rescue for breast implant complications. *Breast J* 2010;16:169–75.
- [19] Rubin JP, Coon D, Zuley M, Toy J, Asano Y, Kurita M, et al. Mammographic changes after fat transfer to the breast compared with changes after breast reduction: a blinded study. *Plast Reconstr Surg* 2012;129:1029–38.
- [20] Perin EC, Sanz-Ruiz R, Sánchez PL, Lasso J, Pérez-Cano R, Alonso-Farto JC, et al. Adipose-derived regenerative cells in patients with ischemic cardiomyopathy: the PRECISE Trial. *Am Heart J* 2014;168:88–95.
- [21] Sakai Y, Takamura M, Seki A, Sunagozaka H, Terashima T, Komura T, et al. Phase I clinical study of liver regenerative therapy for cirrhosis by intrahepatic arterial infusion of freshly isolated autologous adiposetissue-derived stromal/stem (regenerative) cell. *Regen Ther* 2017;6:52–64.
- [22] Omura S, Mizuki N, Kawabe R, Ota S, Kobayashi S, Fujita K. A carrier for clinical use of recombinant human BMP-2: dehydrothermally cross-linked composite of fibrillar and denatured atelocollagen sponge. *Int J Oral Maxillofac Surg* 1998;27:129–34.
- [23] Tanaka Y, Yamaoka H, Nishizawa S, Nagata S, Ogasawara T, Asawa Y, et al. The optimization of porous polymeric scaffolds for chondrocyte/atelocollagen based tissue-engineered cartilage. *Biomaterials* 2010;31:4506–16.
- [24] Zhang ZZ, Jiang D, Ding JX, Wang SJ, Zhang L, Zhang JY, et al. Role of scaffold mean pore size in meniscus regeneration. *Acta Biomater* 2016;43:314–26.
- [25] Ozeki N, Muneta T, Koga H, Katagiri H, Otabe K, Okuno M, et al. Transplantation of Achilles tendon treated with bone morphogenetic protein 7 promotes meniscus regeneration in a rat model of massive meniscal defect. *Arthritis Rheum* 2013;65:2876–86.
- [26] Shibata Y, Suzuki D, Wurihan, Yamada A, Maruyama N, Fujisawa N, et al. Lysyl oxidase like-2 reinforces unsatisfactory ossification induced by bone morphogenetic protein-2: relating nanomechanical properties and molecular changes. *Nanomedicine* 2013;9:1036–47.
- [27] Storm C, Pastore JJ, MacKintosh FC, Lubensky TC, Janmey PA. Nonlinear elasticity in biological gels. *Nature* 2005;435:191–4.
- [28] Maruyama N, Shibata Y, Wurihan, Swain MV, Kataoka Y, Takiguchi Y, et al. Strain-rate stiffening of cortical bone: observations and implications from nanoindentation experiments. *Nanoscale* 2014;6:14863–71.
- [29] Maruyama N, Shibata Y, Mochizuki A, Yamada A, Maki K, Inoue T, et al. Bone micro-fragility caused by the mimetic aging processes in α -klotho deficient mice: in situ nanoindentation assessment of dilatational bands. *Biomaterials* 2015;47:62–71.
- [30] Katagiri H, Muneta T, Tsuji K, Horie M, Koga H, Ozeki N, et al. Transplantation of aggregates of synovial mesenchymal stem cells regenerates meniscus more effectively in a rat massive meniscal defect. *Biochem Biophys Res Commun* 2013;435:603–9.
- [31] Bhargava MM, Attia ET, Murrell GA, Dolan MM, Warren RF, Hannafin JA. The effect of cytokines on the proliferation and migration of bovine meniscal cells. *Am J Sports Med* 1999;27:636–43.
- [32] Pangborn CA, Athanasiou KA. Growth factors and fibrochondrocytes in scaffolds. *J Orthop Res* 2005;23:1184–90.
- [33] Speirs AD, Beaulé PE, Ferguson SJ, Frei H. Stress distribution and consolidation in cartilage constituents is influenced by cyclic loading and osteoarthritic degeneration. *J Biomech* 2014;47:2348–53.
- [34] Makris EA, Hadidi P, Athanasiou KA. The knee meniscus: structure-function, pathophysiology, current repair techniques, and prospects for regeneration. *Biomaterials* 2011;32:7411–31.
- [35] Wenchang T, Wenxiao P, Mingyu X. A note on unsteady flows of a viscoelastic fluid with the fractional Maxwell model between two parallel plates. *Int J Non Linear Mech* 2003;38:645–50.
- [36] Tan GK, Dinnes DLM, Butler LN, Cooper-White JJ. Interactions between meniscal cells and a self-assembled biomimetic surface composed of hyaluronic acid, chitosan and meniscal extracellular matrix molecules. *Biomaterials* 2010;31:6104–18.